

# Sensing-Constrained Diversity-Multiplexing Tradeoff in MIMO ISAC: A Geometric Approach

Yinuo Du\*, Ziping Lu\*, Xiao Shen\*, Hanying Zhao†, and Yuan Shen\*

\*Department of Electronic Engineering, BNRist, Tsinghua University, Beijing, China

†Division of Information Science and Engineering, KTH Royal Institute of Technology, Stockholm, Sweden  
Email: {duyn24, lzp23, shenx20}@mails.tsinghua.edu.cn, hanying@kth.se, shenyuan\_ee@tsinghua.edu.cn

**Abstract**—Diversity and multiplexing are the two fundamental gains of multiple-input and multiple-output (MIMO) communications, enabling systems to simultaneously achieve increased reliability and higher data rates. The intricate interplay between these two metrics is captured by the celebrated diversity-multiplexing tradeoff (DMT). With the rapid evolution of wireless technologies, low-latency integrated sensing and communication (ISAC) has emerged as a key enabler for 6G applications, including extended reality (XR) and massive digital twins. Consequently, understanding the DMT within MIMO ISAC systems becomes critical. In this paper, we investigate the communication DMT in a mono-static MIMO ISAC system under Rayleigh fading, specifically when the transmitter is constrained to emit sensing-optimal waveforms. By unveiling the geometric properties of generalized Stiefel manifolds and employing large-deviation analysis, we characterize the asymptotic outage probability of this typical ISAC channel. This formulation yields an elegant converse bound on the sensing-constrained DMT. Ultimately, our work provides an answer to a pivotal unanswered question in ISAC system design: How much MIMO gain is fundamentally sacrificed in communication to integrate optimal sensing capabilities?

**Index Terms**—Integrated sensing and communication, MIMO communication, Diversity-multiplexing tradeoff, Stiefel manifold

## I. INTRODUCTION

Recognized as a pivotal technology for 6G [1], integrated sensing and communication (ISAC) outperforms traditional separated designs by efficiently sharing hardware and spectral resources [2]. To fully realize its potential, multiple-input and multiple-output (MIMO) technology is indispensable: it endows the system with high spatial resolution for sensing while unlocking critical diversity and multiplexing gains for communication [3]. Consequently, MIMO ISAC has emerged as a cornerstone for next-generation applications such as autonomous vehicular networks and digital twins.

Link-level ISAC encompasses two primary paradigms: mono-static [2], [4], where Tx performs sensing using known codewords, and bi-static [5], where Rx jointly senses and decodes. Due to Tx’s perfect knowledge of the transmitted signals, the mono-static approach achieves superior sensing accuracy and is thus of greater practical interest [3]. Theoretically, ISAC is studied under either the infinite blocklength assumption [2], [4] using Shannon capacity, or the finite blocklength regime [5] where decoding error probabilities are strictly non-zero. Since 6G targets ultra-low latency [1] and sensing is inherently time-sensitive, this paper specifically

investigates a mono-static MIMO ISAC channel within the finite blocklength regime.

In MIMO communications, the fundamental interplay between reliability and data rates is elegantly captured by the diversity-multiplexing tradeoff (DMT) [6]. For MIMO ISAC systems, the theoretical sensing-communication tradeoff has been recently established using the Cramér-Rao bound (CRB) and achievable rate [2]. However, this ergodic, zero-error formulation is incompatible with 6G applications such as hyper-reliable and low-latency communications (HRLLC) and neglects the diversity gain brought by MIMO. Consequently, to reflect the finite-blocklength realities of practical MIMO ISAC systems, characterizing the sensing-communication tradeoff directly through the DMT framework is of critical importance.

This paper investigates the communication DMT of a mono-static MIMO ISAC Rayleigh fading channel in the finite-blocklength regime. Under the strict constraint of emitting sensing-optimal waveforms, transmit codewords are geometrically confined to a generalized Stiefel manifold. Leveraging Riemannian geometry and large-deviation analysis, we characterize the asymptotic outage probability to derive an elegant converse bound on the sensing-constrained DMT. Ultimately, we provide a preliminary answer to the pivotal unanswered question in MIMO ISAC: How much MIMO communication gain must be sacrificed to guarantee optimal sensing?

*Notations:* Random variables, vectors, and matrices are denoted by  $x$ ,  $\mathbf{x}$ , and  $\mathbf{X}$ , with their respective realizations given by  $x$ ,  $\mathbf{x}$ , and  $\mathbf{X}$ . For a vector  $\mathbf{x}$ ,  $\mathbf{x}_{a:b}$  denotes the vector  $(x_a, x_{a+1}, \dots, x_b)$ . The relation  $a(x) \stackrel{\geq}{\leq} b(x)$  signifies that  $\lim_{x \rightarrow \infty} a(x)/b(x) \stackrel{\geq}{\leq} 1$ . We also use  $(\cdot)^+ \triangleq \max\{0, \cdot\}$ .

## II. PROBLEM FORMULATION

### A. MIMO ISAC Model and Scheme

We consider a mono-static MIMO ISAC system where a base station (BS) down-link communicates to a user equipment (UE) while simultaneously performing radar sensing. The BS is equipped with  $M$  Tx antennas and  $N_s$  Rx antennas, whereas the UE is equipped with  $N_c$  Rx antennas. Specifically, the sensing and communication (S&C) channels are given by:

$$\begin{cases} \mathbf{Y}_s = \sqrt{\eta_s/M} \mathbf{H}_s \mathbf{X} + \mathbf{Z}_s, & (1a) \\ \mathbf{Y}_c = \sqrt{\eta_c/M} \mathbf{H}_c \mathbf{X} + \mathbf{Z}_c & (1b) \end{cases}$$

where  $\mathbf{Y}_s$  and  $\mathbf{Y}_c$  denote the received S&C signals, and  $\mathbf{X} \in \mathbb{C}^{M \times T}$  is the transmitted ISAC codeword over a blocklength of  $T \geq M$ .  $\mathbf{H}_s = \mathbf{G}(\boldsymbol{\eta}) \in \mathbb{C}^{N_s \times M}$  represents the sensing channel response uniquely determined by a latent random parameter  $\boldsymbol{\eta} \in \mathbb{R}^K$  via an injective mapping  $\mathbf{G}(\cdot)$ . The communication channel  $\mathbf{H}_c \in \mathbb{C}^{N_c \times M}$  undergoes quasi-static Rayleigh fading and is assumed to be independent of  $\mathbf{H}_s$ . The terms  $\mathbf{Z}_s$  and  $\mathbf{Z}_c$  represent additive white Gaussian noise. Without loss of generality, we assume  $\mathbf{X}, \mathbf{H}_s, \mathbf{H}_c$  have normalized power, i.e.  $\mathbb{E}(\text{tr}(\mathbf{X}\mathbf{X}^H))/MT = \mathbb{E}(\text{tr}(\mathbf{H}_s\mathbf{H}_s^H))/N_sM = 1$ , and the entries of  $\mathbf{H}_c, \mathbf{Z}_s$ , and  $\mathbf{Z}_c$  are modeled as i.i.d.  $\mathcal{CN}(0, 1)$ . Under these normalizations,  $\eta_s$  and  $\eta_c$  define the receive signal-to-noise ratios (SNRs) at the sensing Rx and UE, respectively.

For an ISAC transmission, the BS first selects a message  $j$  uniformly from the set  $\mathcal{J} = \{1, 2, \dots, J\}$  and maps  $j$  to a codeword  $\mathbf{X} = \boldsymbol{\mu}(j)$  from the codebook  $\mathcal{X} \subset \mathbb{C}^{M \times T}$ , where  $\boldsymbol{\mu}: \mathcal{J} \rightarrow \mathcal{X}$  is the bijective encoder. Finally,  $\mathbf{X}$  is transmitted through the wireless channel (1) to the S&C receivers.

At the communication receiver, we assume a coherent scheme where the channel matrix  $\mathbf{H}_c$  is known to the UE. Upon receiving  $\mathbf{Y}_c$ , the UE estimates the transmitted message as  $\hat{j} = \gamma(\mathbf{Y}_c, \mathbf{H}_c) \in \mathcal{J}$ , where  $\gamma: \mathbb{C}^{N_c \times T} \times \mathbb{C}^{N_c \times M} \rightarrow \mathcal{J}$  denotes the communication decoding function.

At the sensing receiver, the latent parameter  $\boldsymbol{\eta}$  is estimated using both the received signal  $\mathbf{Y}_s$  and the known transmitted codeword  $\mathbf{X}$ . This process yields the estimate  $\hat{\boldsymbol{\eta}} = \omega(\mathbf{Y}_s, \mathbf{X})$ , where  $\omega: \mathbb{C}^{N_s \times T} \times \mathcal{X} \rightarrow \mathbb{R}^K$  defines the estimation function.

*Remark 1:* The sensing channel model (1a) has been used in the seminal work [2], whereas we further assume that the communication channel (1b) falls under Rayleigh fading. As illustrated in Fig. 1, such S&C channel models are of particular practical interest in complex urban scenarios such as low-altitude aerial networks, where target sensing is dominated by strong line-of-sight (LOS) radar echoes while the communication link to the UE suffers from severe scattered fading.

### B. S&C Evaluation Metrics

To evaluate sensing performance, we adopt the Miller-Chang-type Bayesian Cramér-Rao bound (BCRB). Specifically, by defining the conditional Bayesian Fisher information matrix (BFIM) as

$$\mathbf{J}_{\boldsymbol{\eta}|\mathbf{X}} \triangleq \mathbb{E}_{\mathbf{Y}_s, \boldsymbol{\eta}|\mathbf{X}} \left[ [\partial \ln p(\mathbf{Y}_s|\mathbf{X}, \boldsymbol{\eta}) / \partial \boldsymbol{\eta}] [\partial \ln p(\mathbf{Y}_s|\mathbf{X}, \boldsymbol{\eta}) / \partial \boldsymbol{\eta}]^T \right] + \mathbb{E}_{\boldsymbol{\eta}} \left[ [\partial \ln p(\boldsymbol{\eta}) / \partial \boldsymbol{\eta}] [\partial \ln p(\boldsymbol{\eta}) / \partial \boldsymbol{\eta}]^T \right], \quad (2)$$

the corresponding Cramér-Rao inequality is given by:

$$\mathbb{E}(\|\hat{\boldsymbol{\eta}} - \boldsymbol{\eta}\|_2^2) \geq \mathbb{E}_{\mathbf{X}} \left[ \text{tr} \left( \mathbf{J}_{\boldsymbol{\eta}|\mathbf{X}}^{-1} \right) \right] \triangleq e, \quad (3)$$

where  $e$  denotes the BCRB for the mean squared error (MSE) of the latent parameter  $\boldsymbol{\eta}$ .

For communication performance, there exist two fundamental metrics: the transmission rate  $R \triangleq (\log J)/T$  and the decoding error probability  $P_e = \mathbb{P}(\hat{j} \neq j)$ . In an ergodic channel with infinite code length,  $P_e$  is irrelevant as

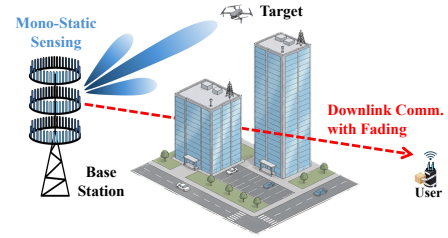


Fig. 1. Illustration of a typical mono-static MIMO ISAC scenario.

Shannon capacity can be used. However, this obscures the critical MIMO diversity gains. Therefore, we evaluate the communication link through the rigorous lens of diversity and multiplexing gains [6]. Specifically, an ISAC scheme achieves a multiplexing gain  $r \geq 0$  and a diversity gain  $d \geq 0$  if

$$\lim_{\eta_c \rightarrow \infty} R / \log \eta_c = r, \quad - \lim_{\eta_c \rightarrow \infty} \log P_e / \log \eta_c = d. \quad (4)$$

In MIMO systems, the fundamental interplay between these two gains is characterized by the DMT. Let  $d^*(r)$  denote the optimal DMT curve, which represents the supremum of achievable diversity gains for any target multiplexing gain  $r$ .

### C. S&C Optimal Waveform Design

Next, we consider the dedicated optimal waveforms that strictly focus on either the sensing channel (1a) or the communication channel (1b). For sensing, the optimal waveform aims to minimize the BCRB  $e$ . As demonstrated in [2], this metric is determined solely by the sample covariance matrix of the transmitted signal:

$$\mathbf{R}_{\mathbf{X}} \triangleq T^{-1} \mathbf{X}\mathbf{X}^H. \quad (5)$$

Under mild regularity conditions [2, Prop. 3-5], the optimal sensing covariance is deterministic, i.e.,  $\mathbf{R}_{\mathbf{X}} = \mathbf{R}$ . To facilitate our analysis, we always assume the existence of a unique optimal  $\mathbf{R}$ . Consequently, any sensing-optimal waveform must reside within the set  $\{\mathbf{X} : \mathbf{X}\mathbf{X}^H = T\mathbf{R}\}$ .

Conversely, for the communication link, the optimal waveform achieves the unconstrained DMT  $d^*(r)$ . Provided that  $T \geq M + N_c - 1$ , this optimal tradeoff is achieved by isotropic Gaussian codewords, i.e.,  $\text{vec}(\mathbf{X}) \sim \mathcal{CN}(\mathbf{0}, \mathbf{I}_{MT})$ . The resulting optimal DMT curve  $d^*(r)$  is the well-known piecewise-linear function [6] connecting the points  $(k, d^*(k))$  for  $k = 0, \dots, \min\{M, N_c\}$ , where

$$d^*(k) = (M - k)(N_c - k). \quad (6)$$

By substituting this communication-optimal Gaussian waveform into (2) and (3), its corresponding sensing performance can be readily evaluated. However, characterizing the communication DMT when strictly employing sensing-optimal codewords is highly non-trivial. In the remainder of this paper, we leverage Riemannian geometry to tackle this challenging problem, ultimately deriving a converse bound on the sensing-constrained DMT, denoted as  $d_{\mathbf{R}}^*(r)$ .

### III. DMT WITH OPTIMAL SENSING WAVEFORM

In this section, we establish the main result of this paper: deriving a converse bound on the sensing-constrained DMT  $d_{\mathbf{R}}^*(r)$  via outage analysis under the sensing-optimal condition  $\mathbf{X}\mathbf{X}^H = T\mathbf{R}$ . Fortunately, this constraint defines a smooth manifold in  $\mathbb{C}^{M \times T}$ , belonging to a broader family of generalized Stiefel manifolds formally defined below:

*Definition 1:* For a Hermitian matrix  $\mathbf{0} \preceq \mathbf{A} \in \mathbb{C}^{k \times k}$  and an integer  $n > \text{rk}(\mathbf{A})$ , a generalized Stiefel manifold is

$$S_{\mathbf{A}}^{(k,n)} \triangleq \{\mathbf{X} \in \mathbb{C}^{k \times n}, \mathbf{X}\mathbf{X}^H = \mathbf{A}\} \quad (7)$$

which forms a smooth real manifold of dimension  $\text{rk}(\mathbf{A})(2n - \text{rk}(\mathbf{A}))$ . Notably, the standard complex Stiefel manifold [7] is recovered as the special case  $S_{\mathbf{I}_k}^{(k,n)}$ .

For subsequent analysis, we also recall the unitary Lie group of degree  $n$ , given by  $U(n) \triangleq \{U \in \mathbb{C}^{n \times n} \mid \mathbf{U}\mathbf{U}^H = \mathbf{I}_n\} = S_{\mathbf{I}_n}^{(n,n)}$ . Crucially,  $U(n)$  exerts a smooth and transitive group action on  $S_{\mathbf{A}}^{(k,n)}$  via right matrix multiplication.

In this work, we endow the generalized Stiefel manifolds with the standard Euclidean metric. That is, for any tangent vectors  $\Delta_1, \Delta_2$  in the tangent space  $T_{\mathbf{S}}S_{\mathbf{A}}^{(k,n)}$  of  $\mathbf{S} \in S_{\mathbf{A}}^{(k,n)}$ , the metric tensor is given by  $g(\Delta_1, \Delta_2) \triangleq \Re\{\text{tr}(\Delta_1 \Delta_2^H)\}$ . The corresponding Euclidean volume measure on  $S_{\mathbf{A}}^{(k,n)}$  is denoted as  $\text{Vol}(\cdot)$ .

Generalized Stiefel manifolds possess several pivotal geometric properties that underpin our analysis:

*Proposition 1 (Properties of  $S_{\mathbf{A}}^{(k,n)}$ ):*

- (a)  $S_{\mathbf{A}}^{(k,n)}$  is a  $U(n)$ -homogeneous space. The metric  $g(\cdot, \cdot)$  and measure  $\text{Vol}(\cdot)$  are  $U(n)$ -invariant. The uniform probability measure  $P_{\mathbf{H}}(\cdot) \triangleq \text{Vol}(\cdot)/\text{Vol}(S_{\mathbf{A}}^{(k,n)})$  is the unique  $U(n)$ -invariant probability measure (Haar measure).
- (b) Let random matrix  $\mathbf{F}$  distributed according to  $P_{\mathbf{H}}$  on  $S_{\mathbf{A}}^{(k,n)}$ . For any  $\mathbf{K} \in \mathbb{C}^{m \times k}$ ,  $\mathbf{K}\mathbf{F} \sim P_{\mathbf{H}}$  on  $S_{\mathbf{K}\mathbf{A}\mathbf{K}^H}^{(m,n)}$ .

*Proof:* See Appendix A.  $\square$

With the geometric perspective, to transmit sensing-optimal codewords is to transmit on a generalized Stiefel manifold and, given a channel realization  $\mathbf{H}_c$ , the noiseless received communication signal also lies on such a manifold, i.e.

$$\mathbf{X} \in S_{T\mathbf{R}}^{(M,T)}, \quad \sqrt{\eta_c/M}\mathbf{H}_c\mathbf{X} \in S_{\eta_c T \mathbf{H}_c \mathbf{R} \mathbf{H}_c^H / M}^{(N_c, T)} \quad (8)$$

To derive a converse bound on the DMT under optimal sensing constraints, we follow the methodology established in the seminal work [6] by first characterizing the outage probability in the high-SNR regime.

#### A. Outage Characterization

In this subsection, we analyze the communication outage for the quasi-static fading channel

$$\mathbf{Y}_{c,t} = \sqrt{\eta_c/M}\mathbf{H}_c\mathbf{X}_t + \mathbf{Z}_c, \quad t = 1, 2, \dots \quad (9)$$

where infinite blocks are transmitted via the same fading channel  $\mathbf{H}_c$ , and each block is constrained on the sensing-optimal manifold, i.e.,  $\mathbf{X}_t \in S_{T\mathbf{R}}^{(M,T)}$ . Omitting subscript  $t$  for brevity, the outage probability at target rate  $R$  is:

$$P_{\text{out}}(R) = \min_{\mathbf{P}_{\mathbf{X}}; \mathbf{X} \perp \mathbf{H}_c} \{\mathbb{P}_{\mathbf{H}_c} (I_{\mathbf{H}_c}(\mathbf{X}; \mathbf{Y}_c) < TR)\}. \quad (10)$$

where  $\perp$  denotes the independence of random variables.  $I_{\mathbf{H}_c}(\mathbf{X}; \mathbf{Y}_c)$  signifies the mutual information conditioned on a fixed realization  $\mathbf{H}_c$ , whereas  $I_{\mathbf{H}_c}(\mathbf{X}; \mathbf{Y}_c)$  represents the associated random variable<sup>1</sup>.

To calculate (10), we have

$$\begin{aligned} I_{\mathbf{H}_c}(\mathbf{X}; \mathbf{Y}_c) &= h_{\mathbf{H}_c}(\mathbf{Y}_c) - h_{\mathbf{H}_c}(\mathbf{Y}_c | \mathbf{X}) \\ &= h\left(\sqrt{\eta_c/M}\mathbf{H}_c\mathbf{X} + \mathbf{Z}_c\right) - N_c T \log(\pi e). \end{aligned} \quad (11)$$

Note that  $\sqrt{\eta_c/M}\mathbf{H}_c\mathbf{X} \in S_{\eta_c T \mathbf{H}_c \mathbf{R} \mathbf{H}_c^H / M}^{(N_c, T)}$  by (8).

Using Proposition 1, since  $S_{\eta_c T \mathbf{H}_c \mathbf{R} \mathbf{H}_c^H / M}^{(N_c, T)}$  is homogeneous, uniform distribution  $P_{\mathbf{H}}$  should maximize  $I_{\mathbf{H}_c}(\mathbf{X}; \mathbf{Y}_c)$ , which can be achieved by choosing  $\mathbf{X} \sim P_{\mathbf{H}}$  regardless of  $\mathbf{H}_c$ . Following this intuition, we arrive at the following proposition.

*Proposition 2:* The maximum mutual information (11) and the outage probability (10) are obtained by  $P_{\mathbf{H}}$ , i.e.,  $P_{\mathbf{H}} = \arg\max_{\mathbf{P}_{\mathbf{X}}} [I_{\mathbf{H}_c}(\mathbf{X}; \mathbf{Y}_c)] = \arg\min_{\mathbf{P}_{\mathbf{X}}; \mathbf{X} \perp \mathbf{H}_c} \{\mathbb{P}_{\mathbf{H}_c} (I_{\mathbf{H}_c}(\mathbf{X}; \mathbf{Y}_c) < TR)\}$ .<sup>2</sup>

*Proof:* See Appendix B.  $\square$

For a smooth Euclidean submanifold, [8] finds that at high SNR, the optimal distribution is asymptotically uniform. In our case, we proved  $P_{\mathbf{H}}$  achieves the maximal entropy regardless of SNR level. Therefore, we always set  $\mathbf{X} \sim P_{\mathbf{H}}$  on  $S_{T\mathbf{R}}^{(M,T)}$ .

Next, we apply the singular value decomposition (SVD) to decompose  $\mathbf{H}_c\mathbf{X}$ , effectively transforming the Rx manifold into a canonical form. For brevity, we consider the case where  $\text{rk}(\mathbf{R}) \leq N_c$  and  $T \geq N_c$ .

By compact SVD, we have the decomposition  $\mathbf{H}_c\mathbf{X}/\sqrt{T} = \mathbf{V}\Sigma\mathbf{W}$ , with  $\mathbf{V} \in U(N_c)$ ,  $\Sigma \in \mathbb{R}^{N_c \times N_c}$  and  $\mathbf{W} \in S_{\mathbf{I}_{N_c}}^{(N_c, T)}$ . Let  $\Sigma = \text{diag}(\sigma_1, \dots, \sigma_{\text{rk}(\mathbf{R})}, \mathbf{0}) \triangleq \text{diag}(\sigma^T, \mathbf{0})$  and  $\sigma_1 \geq \dots \geq \sigma_{\text{rk}(\mathbf{R})} \geq 0$ .  $\mathbf{V}, \Sigma$  are functions of  $\mathbf{H}_c$  by eigendecomposition  $\mathbf{H}_c \mathbf{R} \mathbf{H}_c^H = \mathbf{V} \Sigma \mathbf{V}^H$ . Since  $|\det \mathbf{V}| = 1$ , we have

$$h\left(\sqrt{\eta_c/M}\mathbf{H}_c\mathbf{X} + \mathbf{Z}_c\right) = h\left(\sqrt{\eta_c T/M}\Sigma\mathbf{W} + \mathbf{Z}_c\right) \quad (12a)$$

$$I_{\mathbf{H}_c}(\mathbf{X}; \mathbf{Y}_c) = I_{\sigma}(\mathbf{C} + \mathbf{Z}_c; \mathbf{W}) \quad (12b)$$

where  $\mathbf{C} \triangleq \sqrt{\eta_c T/M}\Sigma\mathbf{W}$ . By Proposition 1-b, the uniform distribution of  $\mathbf{X}$  ensures that  $\mathbf{W}$  and  $\mathbf{C}$  are uniformly distributed on  $S_{\mathbf{I}_{N_c}}^{(N_c, T)}$  and  $S_{\eta_c T \Sigma^2 / M}^{(N_c, T)}$ , respectively. Consequently, the mutual information and the outage probability (10) are entirely characterized by the geometry of the manifold  $S_{\eta_c T \Sigma^2 / M}^{(N_c, T)}$ , whose ‘‘shape’’ depends on the SNR  $\eta_c$  and the singular values  $\sigma$ .

To facilitate geometric intuition, we define the log-singular value  $\alpha_i \triangleq -\log \sigma_i / \log \eta_c$ , and use  $\boldsymbol{\alpha} \triangleq (\alpha_1, \dots, \alpha_{\text{rk}(\mathbf{R})})$ ,  $\alpha_1 \leq \dots \leq \alpha_{\text{rk}(\mathbf{R})}$ . By the definition of  $\mathbf{C}$ , we have

$$\mathbf{C} = \sqrt{T/M} \text{diag}\left(\eta_c^{0.5-\alpha_1}, \dots, \eta_c^{0.5-\alpha_{\text{rk}(\mathbf{R})}}, 0, \dots, 0\right) \mathbf{W}. \quad (13)$$

<sup>1</sup>This notational convention for distinguishing between specific realizations and their corresponding random variables is maintained throughout the remainder of this paper without further explicit mention.

<sup>2</sup>This result is also latently used in [2] as a conjecture.

$$c_{\eta_c, \alpha} \triangleq \max \left\{ \max_{\mathbf{S} \in S_{\eta_c, \alpha}, \Delta \in \mathcal{T}_{\mathbf{S}} S_{\eta_c, \alpha}, g(\Delta, \Delta) = 1} |\mathbf{II}_{\mathbf{S}}(\Delta, \Delta)|, \rho_{\perp}(S_{\eta_c, \alpha})^{-1}, \rho_{\top}(S_{\eta_c, \alpha})^{-1} \right\} \quad (16)$$

$$|h(\mathbf{C}_1 + \mathbf{Z}_{c1}) - m^2 \log(\pi e)/2 - \log \text{Vol}(S_{\eta_c, \alpha})| \leq \text{const}(m, T) \delta^{-1} (1 + c_{\eta_c, \alpha} \eta_c^{0.5})^{\delta} c_{\eta_c, \alpha}^2 \log^2(c_{\eta_c, \alpha}) \quad (17)$$

Since  $\mathbf{W}$  is uniform on the standard Stiefel manifold  $S_{I_{N_c}^{(N_c, T)}}$ , (13) characterizes an ‘‘inflation’’ process in  $\mathbb{C}^{N_c \times T}$ . Specifically, while the rising SNR drives a polynomial expansion of the generalized Stiefel manifold with an exponential order of 0.5, the channel  $\mathbf{H}_c$  moderates this growth by reducing the expansion order by  $\alpha_i$ . When the composite channel  $\mathbf{H}_c \mathbf{X}$  exhibits atypically small singular values (i.e., high  $\alpha_i$ ), the manifold  $S_{\eta_c T \Sigma^2/M}$  wouldn’t be inflated enough to support reliable communication, that is when the outage event appears, i.e., the channel realization  $\mathbf{H}_c$  is in ‘‘deep fade’’ [6].

By (12b), the outage probability (10) can be reformulated as

$$P_{\text{out}}(R) = \mathbb{P}_{\alpha} (I_{\alpha}(\mathbf{C} + \mathbf{Z}_c; \mathbf{W}) < TR). \quad (14)$$

To derive an asymptotic result for (14), we first characterize  $I_{\alpha}(\mathbf{C} + \mathbf{Z}_c; \mathbf{W})$  with a fixed  $\alpha$  in the high-SNR regime.

### B. Asymptotic Mutual Information

In this subsection, we characterize the asymptotic mutual information for a fixed realization  $\alpha$  as  $\eta_c \rightarrow \infty$ . Per (13), the manifold expansion rate is governed by the exponents  $\{0.5 - \alpha_i\}$ . For dimensions where  $\alpha_i \geq 0.5$ , the manifold fails to expand w.r.t.  $\eta_c$ , implying that effective communication is predominantly supported by the subset of dimensions satisfying  $\alpha_i < 0.5$ . We define  $m \triangleq |\{i \mid \alpha_i < 0.5\}|$  as the number of such dominant dimensions. Since  $m = 0$  results in a trivially bounded mutual information, we focus on  $m > 0$  throughout this section, where  $\alpha_m$  denotes the largest log-singular value satisfying  $\alpha_i < 0.5$ . Our geometric intuition is formalized in the following proposition.

*Proposition 3:* Given  $\alpha$ , define  $\mathbf{W}_1 \sim P_{\mathbf{H}}$  on  $S_{I_m^{(m, T)}}$  and let  $\mathbf{Z}_{c1} \in \mathbb{C}^{m \times T}$  be a noise matrix with i.i.d.  $\mathcal{CN}(0, 1)$  entries. The following asymptotic equivalence holds:

$$\lim_{\eta_c \rightarrow \infty} \frac{I_{\alpha} \left( \sqrt{T/M} \text{diag}(\eta_c^{0.5 - \alpha_{1:m}}) \mathbf{W}_1 + \mathbf{Z}_{c1}; \mathbf{W}_1 \right)}{I_{\alpha}(\mathbf{C} + \mathbf{Z}_c; \mathbf{W})} = 1. \quad (15)$$

*Proof:* See Appendix C.  $\square$

Proposition 3 implies that the asymptotic mutual information is determined solely by the log-singular values  $\alpha_{1:m}$ , corresponding to the first  $m$  rows of  $\mathbf{C}$  that expand at a positive rate according to (13). Define the reduced-dimension noiseless component as

$$\mathbf{C}_1 \triangleq \sqrt{T/M} \text{diag}(\eta_c^{0.5 - \alpha_{1:m}}) \mathbf{W}_1 \quad (18)$$

which is uniformly distributed on the manifold  $S_{\eta_c, \alpha} \triangleq S_{\frac{T}{M} \text{diag}(\eta_c^{1 - 2\alpha_{1:m}})}$  by Proposition 1-b. In the high-SNR regime, the outage probability (14) satisfies

$$P_{\text{out}}(R) \doteq \mathbb{P}_{\alpha} (h_{\alpha}(\mathbf{C}_1 + \mathbf{Z}_{c1}) < T(R + m \log(\pi e))). \quad (19)$$

As shown in (19), the asymptotic outage is governed by the differential entropy of a uniform distribution over the inflating manifold  $S_{\eta_c, \alpha}$  perturbed by normalized additive noise  $\mathbf{Z}_{c1}$ .

Previous literature, such as [2], utilized Weyl’s tube formula [9] to approximate similar but simpler entropy terms. Specifically, [2, Thm. 1] characterized the maximal differential entropy  $h_{\mathbf{H}_c}(\mathbf{C}_x + \mathbf{Z}_{cx})$  for  $\mathbf{C}_x \in S_{\eta_c T \mathbf{H}_c \mathbf{R} \mathbf{H}_c^{\#}/M}$  as  $\eta_c \rightarrow \infty$ . This was achieved by approximating the noise distribution normal to the manifold and assuming uniformity on the surface of every  $\epsilon$ -tube. However, since  $S_{\eta_c, \alpha}$  exhibits row-dependent expansion rates  $\eta_c^{0.5 - \alpha_i}$ , such approximations are inadequate for our rigorous analysis. We thus leverage the formal results in [8], which characterize the entropy of manifold-constrained variables via tubular neighborhood theory. This leads to the following lemma.

*Lemma 1:* Define  $c_{\eta_c, \alpha}$  as in (16), where  $\mathbf{II}_{\mathbf{S}}(\cdot, \cdot)$  is the second fundamental form under Euclidean embedding,  $\rho_{\perp}(\cdot)$  denotes the manifold’s maximal uniform tubular neighborhood radius whereas  $\rho_{\top}(\cdot)$  is the injectivity radius. For any  $\delta \in (0, 1]$ , inequality (17) holds.

*Proof:* This lemma follows from [8, Thm. 4.2.1] by noting that the p.d.f. of  $\mathbf{C}_1$  relative to the volume measure  $\text{Vol}(\cdot)$  is the constant  $(\text{Vol}(S_{\eta_c, \alpha}))^{-1}$ .  $\square$

Lemma 1 establishes that the target entropy is asymptotically approximated by the manifold-entropy  $\log \text{Vol}(S_{\eta_c, \alpha})$ , plus a term  $\frac{1}{2} m^2 \log(\pi e)$  representing the noise contribution within the manifold’s normal bundle. The approximation error is bounded by the RHS of (17), which is determined by  $\eta_c$  and the geometric parameter  $c_{\eta_c, \alpha}$  in (16).  $c_{\eta_c, \alpha}$  integrates three critical geometric properties: the maximum principal curvature  $\max |\mathbf{II}_{\mathbf{S}}(\Delta, \Delta)|$ , the injectivity radius  $\rho_{\top}(S_{\eta_c, \alpha})$ , and the maximal uniform tubular neighborhood radius  $\rho_{\perp}(S_{\eta_c, \alpha})$ . In the following theorem, we show that these quantities vanish at a rate no slower than  $\eta_c^{\alpha_m - 0.5}$ . By selecting an appropriate  $\delta$ , the error term in (17) becomes negligible as  $\eta_c \rightarrow \infty$ .

*Theorem 1 (Asymptotic Mutual Information):* Given  $\alpha$ , the geometric parameter  $c_{\eta_c, \alpha}$  satisfies

$$\lim_{\eta_c \rightarrow \infty} c_{\eta_c, \alpha} \leq \eta_c^{\alpha_m - 0.5}. \quad (20)$$

The corresponding asymptotic differential entropy is given by

$$\lim_{\eta_c \rightarrow \infty} h_{\alpha}(\mathbf{C}_1 + \mathbf{Z}_{c1}) = m^2 \log(\pi e) + \log \text{Vol}(S_{\eta_c, \alpha}). \quad (21)$$

We obtain the following scaling result:

$$\begin{aligned} I_{\mathbf{H}_c}(\mathbf{X}; \mathbf{Y}_c) &\doteq h_{\alpha}(\mathbf{C}_1 + \mathbf{Z}_{c1}) \\ &\doteq \sum_{i=1}^{\text{rk}(\mathbf{R})} (2T + 1 - 2i)(0.5 - \alpha_i)^+ \log(\eta_c). \end{aligned} \quad (22)$$

*Proof:* See Appendix D.  $\square$

*Remark 2:* Theorem 1 establishes the asymptotic mutual information of the compound channel (9) via geometric analysis. For a given realization  $\alpha$ , the mutual information scales with  $\log \eta_c$  with a coefficient of  $\sum_{i=1}^{\text{rk}(\mathbf{R})} (2T+1-2i)(0.5-\alpha_i)^+$ . Consistent with our intuition, only the log-singular values satisfying  $\alpha_i < 0.5$  contribute to the asymptotic growth of  $I_{\mathbf{H}_c}(\mathbf{X}; \mathbf{Y}_c)$ . In the following section, we leverage the distribution of  $\alpha$  to evaluate the asymptotic outage probability and derive a converse bound on the sensing-constrained DMT.

### C. Converse Bound on the Sensing-Constrained DMT

In this section, we first determine the asymptotic outage probability with rate  $r \log \eta_c$  as  $\eta_c \rightarrow \infty$ , i.e.,

$$P_{\text{out}}(r \log \eta_c) \doteq \mathbb{P}_{\alpha} (I_{\alpha}(\mathbf{C}_1 + \mathbf{Z}_{c1}; \mathbf{W}_1) < rT \log \eta_c) \quad (23)$$

Applying Theorem 1 and neglecting boundary sets of measure zero, the outage condition in (23) defines the following region  $\mathcal{A} \subset \mathbb{R}^{\text{rk}(\mathbf{R})}$  in the  $\alpha$ -domain:

$$\mathcal{A} \triangleq \left\{ \alpha_i < \alpha_{i+1}, \sum_{i=1}^{\text{rk}(\mathbf{R})} (2T+1-2i)(0.5-\alpha_i)^+ < Tr \right\} \quad (24)$$

and the asymptotic outage probability is thus:

$$P_{\text{out}}(r \log \eta_c) \doteq \int_{\mathcal{A}} p_{\alpha}(\alpha) d\alpha. \quad (25)$$

The following lemma provides the joint p.d.f.  $p_{\alpha}(\alpha)$  required to evaluate this integral.

*Lemma 2:* Let  $\lambda_1 > \lambda_2 > \dots > \lambda_{\text{rk}(\mathbf{R})} > 0$ <sup>3</sup> be the eigenvalues of the transmit covariance matrix  $\mathbf{R}$ , the joint distribution of  $\alpha = (\alpha_1, \alpha_2, \dots, \alpha_{\text{rk}(\mathbf{R})})^T$  is:

$$p_{\alpha}(\alpha) = F(\eta_c, \text{rk}(\mathbf{R}), N_c, \mathbf{A}_{>0}) \det \left( \left\{ e^{-\eta_c^{-2\alpha_i}} / \lambda_j \right\} \right) \prod_{s=1}^{\text{rk}(\mathbf{R})} \eta_c^{-2\alpha_s(N_c - \text{rk}(\mathbf{R}) + 1)} \prod_{k < l}^{\text{rk}(\mathbf{R})} (\eta_c^{-2\alpha_k} - \eta_c^{-2\alpha_l}) \quad (26)$$

where  $F(\eta_c, \text{rk}(\mathbf{R}), N_c, \mathbf{A}_{>0})$  is the normalizing constant. As  $\eta_c \rightarrow \infty$ ,  $p_{\alpha}(\alpha)$  has the following asymptotic expression

$$\lim_{\eta_c \rightarrow \infty} [\log p_{\alpha}(\alpha) / \log \eta_c] = \begin{cases} -2 \sum_{i=1}^{\text{rk}(\mathbf{R})} (N_c + \text{rk}(\mathbf{R}) + 1 - 2i) \alpha_i, & \alpha_1 > 0 \\ -\infty, & \alpha_1 < 0 \end{cases} \quad (27)$$

*Proof:* See Appendix E.  $\square$

Lemma 2 indicates that if any  $\alpha_i$  falls below zero, the p.d.f. decays super-polynomially. Thus, neglecting the zero-measure boundaries, we focus on the positive orthant  $\mathcal{A}' \triangleq \mathcal{A} \cap (\mathbb{R}^+)^{\text{rk}(\mathbf{R})}$ . The asymptotic outage probability (25) satisfies

$$P_{\text{out}}(r \log \eta_c) \doteq \int_{\mathcal{A}'} \eta_c^{-2 \sum_{i=1}^{\text{rk}(\mathbf{R})} (N_c + \text{rk}(\mathbf{R}) + 1 - 2i) \alpha_i} d\alpha. \quad (28) \\ \doteq \eta_c^{-2 \inf_{\alpha \in \mathcal{A}'} \left( \sum_{i=1}^{\text{rk}(\mathbf{R})} (N_c + \text{rk}(\mathbf{R}) + 1 - 2i) \alpha_i \right)} \triangleq \eta_c^{-d_{\text{rk}(\mathbf{R})}^{\text{out}}}$$

where the second equality utilized Laplace's principle [11].

<sup>3</sup>The eigenvalue distribution of  $\mathbf{H}_c \mathbf{R} \mathbf{H}_c$  is continuous w.r.t.  $\{\lambda_i\}$  [10]. Consequently, (27) readily extends to the case of repeated eigenvalues.

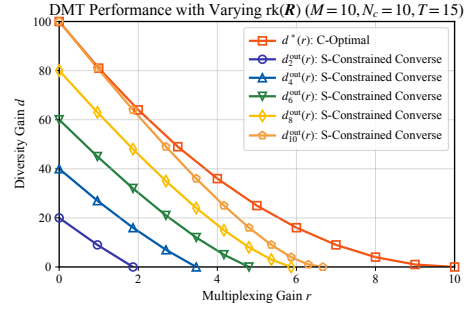


Fig. 2. Impact of  $\text{rk}(\mathbf{R})$  on the sensing-constrained DMT. The converse bound for  $d_{\text{rk}(\mathbf{R})}^{\text{out}}(r)$  also serves as the converse bound in the presence of  $N_c = \text{rk}(\mathbf{R})$  sensing targets in Section IV-A.

Finally, solving for  $d_{\text{rk}(\mathbf{R})}^{\text{out}}$  in (28) characterizes the tradeoff between the asymptotic outage probability  $P_{\text{out}} \doteq \eta_c^{-d_{\text{rk}(\mathbf{R})}^{\text{out}}}$  and the rate  $r \log \eta_c$  for the compound channel (9). This simultaneously provides a converse bound on the sensing-constrained DMT, leading to the main result of this paper.

*Theorem 2:* The outage exponent  $d_{\text{rk}(\mathbf{R})}^{\text{out}}(r)$  is the piecewise-linear function connecting the points  $(r(k), d_{\text{rk}(\mathbf{R})}^{\text{out}}(r(k)))$  for  $k \in \{0, \dots, \text{rk}(\mathbf{R})\}$ , where

$$(r(k), d_{\text{rk}(\mathbf{R})}^{\text{out}}(r(k))) = \left( k \left( 1 - \frac{k}{2T} \right), (N_c - k)(\text{rk}(\mathbf{R}) - k) \right). \quad (29)$$

The function  $d_{\text{rk}(\mathbf{R})}^{\text{out}}(r)$  serves as a converse bound for the sensing-constrained DMT  $d_{\text{R}}^*(r)$ , i.e.,

$$d_{\text{R}}^*(r) \leq d_{\text{rk}(\mathbf{R})}^{\text{out}}(r). \quad (30)$$

*Proof:* See [12, Appendix F].  $\square$

To visualize the implications of Theorem 2, we plot the derived converse bound alongside the original unconstrained communication DMT (6) in Fig. 2. As illustrated, our sensing-constrained bound lies strictly within the original DMT curve. While structurally similar to the piecewise-linear formulation of (6), Theorem 2 reveals a fundamental shift: the performance is dictated by the effective rank  $\text{rk}(\mathbf{R})$  rather than the physical transmit antenna count  $M$ . Consequently, for a fixed  $\text{rk}(\mathbf{R})$ , scaling up  $M$  yields no additional diversity or multiplexing gains. In the full-rank regime ( $\text{rk}(\mathbf{R}) = M$ ), where the bound reaches its maximum, the diversity gain  $(N_c - k)(M - k)$  for a given  $k$  matches the unconstrained case (6). However, the multiplexing gain incurs a penalty of  $k^2/2T$ , fundamentally reflecting the intrinsic loss in communication Degree of Freedom (DoF) necessitated by the sensing constraint.

Evaluating these extreme points yields further insights. At the diversity-optimal point  $(0, N_c \text{rk}(\mathbf{R}))$ , the system incurs no penalty compared to an unconstrained  $\text{rk}(\mathbf{R})$ -antenna MIMO setup. Conversely, the multiplexing-optimal point is  $(\text{rk}(\mathbf{R}) \left( 1 - \frac{\text{rk}(\mathbf{R})}{2T} \right), 0)$ , which aligns perfectly with conventional DoF analysis. Because the transmit signal  $\mathbf{X}$  resides on the generalized Stiefel manifold  $S_{\text{R}}^{(M, T)}$  with  $\text{rk}(\mathbf{R})(2T - \text{rk}(\mathbf{R}))$  real dimensions (DoF), and each real DoF contributes  $1/2T$  to the capacity pre-log factor, our derived multiplexing gain is exactly recovered. This geometric consistency corroborates the tightness of our converse bound.

*Remark 3:* Ultimately, Theorem 2 gives a preliminary answer to the pivotal question posed at the outset. The loss in MIMO gain from transmitting sensing-optimal codewords is twofold: First, the sensing constraint fundamentally restricts the system to  $\text{rk}(\mathbf{R})$  effective Tx dimensions, limiting the entire DMT. Second, compared to an unconstrained system with  $M = \text{rk}(\mathbf{R})$ , although the full spatial diversity is preserved, the multiplexing gain incurs a penalty that grows at higher target rates. Due to space limits, we assume  $\text{rk}(\mathbf{R}) \leq N_c$ ,  $T \geq N_c$ . However, our framework readily generalizes by replacing  $\text{rk}(\mathbf{R})$  with  $\min\{N_c, \text{rk}(\mathbf{R})\}$ . We defer this extension and the achievability bound to future work.

#### IV. CASE STUDY

This section conducts two case studies to gain deeper insights into sensing-constrained MIMO ISAC systems.

##### A. Angle Estimation of Multiple Targets

In this scenario, a sensing BS equipped with  $M = 10$  transmit antennas performs angular estimation on  $N_t$  targets while simultaneously communicating with a UE having  $N_c = 10$  receive antennas. The sensing channel is modeled as

$$\mathbf{H}_s = \sum_{n=1}^{N_t} \beta_n \mathbf{a}(\theta_n) \mathbf{v}^H(\theta_n) \quad (31)$$

where  $\beta_n$  denotes the radar cross-section of the  $n$ -th target,  $\{\theta_n\}_{n=1}^{N_t}$  represents the targets' angular positions, and  $\mathbf{a}(\theta_n)$  and  $\mathbf{v}(\theta_n)$  are the steering vectors of the transmit and sensing receive arrays, respectively. The parameter vector to be estimated is  $\boldsymbol{\eta} = (\theta_1, \dots, \theta_{N_t})$ , with dimension  $K = N_t$ . According to [2, Co. 2], the  $\text{rk}(\mathbf{R})$  satisfies  $\text{rk}(\mathbf{R}) \leq \min\{M, N_t\}$ . Therefore, the sensing-constrained DMT is upper-bounded by  $d_{\mathbf{R}}^*(r) \leq d_{\text{rk}(\mathbf{R})}^{\text{out}}(r) \leq d_{N_t}^{\text{out}}(r)$ . Fig. 2 plots the converse bound  $d_{N_t}^{\text{out}}(r)$  across  $N_t \in \{2, 4, 6, 8, 10\}$ . Counterintuitively, our DMT bound improves as  $N_t$  increases. This phenomenon arises because Rayleigh fading channels inherently benefit from spatially diverse transmissions. While tracking fewer targets restricts the transmit beam to a limited set of spatial directions, a larger target count forces a more uniform spatial spectrum, thereby unlocking additional communication DoF.

##### B. $\mathbf{H}_s$ Estimation

In this scenario, we consider a system with  $M = N_c = 3$  and a varying blocklength  $T$ , where the sensing BS aims to estimate the sensing channel matrix  $\mathbf{H}_s$  directly. Assuming  $\text{vec}(\mathbf{H}_s) \sim \mathcal{CN}(\mathbf{0}, \mathbf{I}_{MN_s})$ , it follows from [2] that the optimal covariance matrix is  $\mathbf{R} = \mathbf{I}$  with  $\text{rk}(\mathbf{R}) = 3$ . The corresponding sensing-constrained DMT bound is illustrated in Fig. 3. As  $T$  increases, the constrained DMT gradually approaches the original DMT. This behavior can also be understood from a DoF perspective: transmitting over the space  $S_{\mathbf{R}}^{(M,T)}$  incurs a penalty of  $M^2$  DoFs per block. Consequently, the DoF loss per symbol is  $M^2/T$ . As  $T$  grows, this fractional loss diminishes, which increases the available communication DoF per symbol and ultimately yields a higher DMT.

This observation highlights another fundamental tradeoff unique to MIMO ISAC systems: the tension between latency

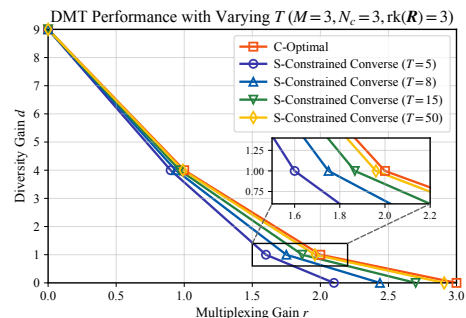


Fig. 3. Impact of  $T$  on the sensing-constrained DMT (see Section IV-B).

and MIMO gain. Unlike the original DMT (6), which is independent of the blocklength  $T$ , our bound reveals that when optimal-sensing capabilities are incorporated, achieving lower latency sacrifices MIMO gain. Conversely, in the latency-unconstrained regime as  $T \rightarrow \infty$ , (29) shows that the sensing-constrained DMT bound converges to the original DMT.

#### V. CONCLUSIONS

This paper investigates the communication DMT of a finite-blocklength MIMO ISAC system constrained to sensing-optimal waveforms. Utilizing Riemannian geometry on generalized Stiefel manifolds and large-deviation analysis, we derive an elegant converse bound on the sensing-constrained DMT. Specifically, this derived bound provides a quantitative characterization of the communication MIMO gain that is traded off to support optimal sensing.

#### REFERENCES

- [1] ITU-R, "Framework and overall objectives of the future development of IMT for 2030 and beyond," International Telecommunication Union (ITU), Geneva, Switzerland, Recommendation (ITU-R M.2160-0) M.2160-0, Nov 2023.
- [2] Y. Xiong, F. Liu, Y. Cui *et al.*, "On the fundamental tradeoff of integrated sensing and communications under Gaussian channels," *IEEE Trans. Inf. Theory*, vol. 69, no. 9, pp. 5723–5751, 2023.
- [3] N. González-Prelcic, M. Furkan Keskin, O. Kallio *et al.*, "The integrated sensing and communication revolution for 6G: Vision, techniques, and applications," *Proc. IEEE*, vol. 112, no. 7, pp. 676–723, 2024.
- [4] M. Ahmadi-pour, M. Kobayashi, M. Wigger, and G. Caire, "An information-theoretic approach to joint sensing and communication," *IEEE Trans. Inf. Theory*, vol. 70, no. 2, pp. 1124–1146, 2022.
- [5] X. Shen, Z. Lu, N. Zhao, H. Zhao, and Y. Shen, "Fundamental tradeoff of bistatic ISAC under Gaussian fading channels at finite blocklength," *IEEE Trans. Inf. Theory*, 2025.
- [6] L. Zheng and D. N. C. Tse, "Diversity and multiplexing: A fundamental tradeoff in multiple-antenna channels," *IEEE Trans. Inf. Theory*, vol. 49, no. 5, pp. 1073–1096, 2003.
- [7] Y. Chikuse, *Statistics on special manifolds*. Springer Science & Business Media, 2003, vol. 174.
- [8] I. Weiner, *High-SNR capacity of AWGN channels with generic alphabet constraints*. Harvard University, 2017.
- [9] H. Weyl, "On the volume of tubes," *American Journal of Mathematics*, vol. 61, no. 2, pp. 461–472, 1939.
- [10] A. M. Tulino and S. Verdú, *Random matrix theory and wireless communications*. Now Publishers Inc, 2004.
- [11] A. Dembo and O. Zeitouni, *Large deviations techniques and applications*. Springer Science & Business Media, 2009, vol. 38.
- [12] Y. Du, Z. Lu, X. Shen, H. Zhao, and Y. Shen, "Sensing-constrained diversity-multiplexing tradeoff in MIMO ISAC: A geometric approach," *arXiv preprint (pending)*, 2026, available at <https://cloud.tsinghua.edu.cn/d/87716b67b6ed49a5aa62/>.

- [13] J. M. Lee, *Introduction to Riemannian manifolds*. Springer, 2018, vol. 2.
- [14] L. Zheng and D. N. C. Tse, "Communication on the Grassmann manifold: A geometric approach to the noncoherent multiple-antenna channel," *IEEE Trans. Inf. Theory*, vol. 48, no. 2, pp. 359–383, 2002.
- [15] A. T. James, "Distributions of matrix variates and latent roots derived from normal samples," *Ann. of Math. Stat.*, vol. 35, no. 2, pp. 475–501, 1964.

APPENDIX A  
PROOF OF PROPOSITION 1

A. Proof of Proposition 1-a

*Proof:* Since  $U(n)$  acts smoothly and transitively on  $S_{\mathbf{A}}^{(k,n)}$ ,  $S_{\mathbf{A}}^{(k,n)}$  is a  $U(n)$ -homogeneous space.

For  $U \in U(n)$ , let  $\Delta_1, \Delta_2 \in \text{T}_{S_{\mathbf{A}}^{(k,n)}}$  for arbitrary  $S \in S_{\mathbf{A}}^{(k,n)}$ . By right-multiplication,  $\Delta_1, \Delta_2$  is pushed forward to  $\Delta_1 U, \Delta_2 U \in \text{T}_{S U} S_{\mathbf{A}}^{(k,n)}$ , since  $g(\Delta_1 U, \Delta_2 U) = \Re\{\text{tr}(\Delta_1 U U^H \Delta_2^H)\} = g(\Delta_1, \Delta_2)$ ,  $g(\cdot, \cdot)$  is  $U(T)$ -invariant, i.e.  $U$  introduces an isometry on  $S_{\mathbf{A}}^{(k,n)}$ .

Correspondingly,  $\text{Vol}(\cdot)$  is also  $U(T)$ -invariant.

Finally, since for a compact homogeneous space there exists, up to a scalar, a unique group-invariant measure, the normalized measure  $P_{\mathbf{H}}(\cdot)$  is the unique  $U(T)$ -invariant probability measure on  $M$ .  $\square$

B. Proof of Proposition 1-b

*Proof:* Since there exists only one unitary-invariant probability measure on the generalized Stiefel manifold, we only need to show that the distribution of  $\mathbf{K}\mathbf{F}$  is  $U(n)$ -invariant.

To prove this, let  $\mu$  denote the probability measure of  $\mathbf{K}\mathbf{F}$  on  $S_{\mathbf{K}\mathbf{A}\mathbf{K}^H}^{(m,n)}$ , for arbitrary Borel set  $E \subset S_{\mathbf{K}\mathbf{A}\mathbf{K}^H}^{(m,n)}$  and arbitrary  $U \in U(n)$ , we have:

$$\begin{aligned} \mu(EU) &= P_{\mathbf{H}}(\mathbf{K}^{-1}(EU)) \stackrel{(a)}{=} P_{\mathbf{H}}(\mathbf{K}^{-1}(E)U) \\ &\stackrel{(b)}{=} P_{\mathbf{H}}(\mathbf{K}^{-1}(E)) = \mu(E) \end{aligned} \quad (32)$$

where (a) comes from the associative property of matrix multiplication and (b) comes from the group-invariance of  $P_{\mathbf{H}}$ . Therefore,  $\mu$  is  $U(n)$ -invariant.  $\square$

APPENDIX B  
PROOF OF PROPOSITION 2

*Proof:* Note that for any  $U \in U(T)$ ,  $|\det U| = 1$ , thus:

$$h(\mathbf{H}_c \mathbf{X}_t + \mathbf{Z}_c) = h[(\mathbf{H}_c \mathbf{X} + \mathbf{Z}_c)U]. \quad (33)$$

Noticing  $\mathbf{X} \perp \mathbf{Z}_t$  and  $\mathbf{Z}_c \sim \mathbf{Z}_c U$ , we have:

$$h(\mathbf{H}_c \mathbf{X}_t + \mathbf{Z}_c) = h(\mathbf{H}_c \mathbf{X}_t U + \mathbf{Z}_c). \quad (34)$$

Consider  $P_{\mathbf{H}}$ , the group-invariant measure on  $U(T)$ , using the concave property of the entropy function,

$$\begin{aligned} h(\mathbf{H}_c \mathbf{X} + \mathbf{Z}_c) &= h[(\mathbf{H}_c \mathbf{X} + \mathbf{Z}_c)U] = \\ &\int_{U(T)} h[(\mathbf{H}_c \mathbf{X} + \mathbf{Z}_c)U] dP_{\mathbf{H}}(U) \leq \\ &h \left[ \int_{U(T)} (\mathbf{H}_c \mathbf{X} + \mathbf{Z}_c)U dP_{\mathbf{H}}(U) \right] = \\ &h \left[ \mathbf{H}_c \int_{U(T)} \mathbf{X}U dP_{\mathbf{H}}(U) + \mathbf{Z}_c \right]. \end{aligned} \quad (35)$$

Since  $\int_{U(T)} \mathbf{X}U dP_{\mathbf{H}}(U) \sim P_{\mathbf{H}}$  on  $S_{T\mathbf{R}}^{(M,T)}$ , we conclude that the optimal distribution is  $P_{\mathbf{H}}$  on  $S_{T\mathbf{R}}^{(M,T)}$ .  $\square$

APPENDIX C  
PROOF OF PROPOSITION 3

*Proof:* For brevity, we use the notation

$$C(\eta_c, \alpha_{1:m}) \triangleq I_{\alpha} \left( \sqrt{\frac{T}{M}} \text{diag}(\eta_c^{0.5-\alpha_{1:m}}) \mathbf{W}_1 + \mathbf{Z}_{c1}; \mathbf{W}_1 \right). \quad (36)$$

Using Proposition 1-b, one can view  $\mathbf{W}_1$  as the first  $m$  rows of  $\mathbf{W}$ , and  $\sqrt{\frac{T}{M}} \text{diag}(\eta_c^{0.5-\alpha_1}, \dots, \eta_c^{0.5-\alpha_m}) \mathbf{W}_1$  as the first  $m$  rows of  $\mathbf{C}$  as they are all uniformly distributed on their corresponding generalized Stiefel manifold.

For the sake of brevity, we use following notations:

$$\mathbf{W} \triangleq (\mathbf{W}_1^H, \mathbf{W}_2^H)^H, \mathbf{C} \triangleq (\mathbf{C}_1^H, \mathbf{C}_2^H)^H, \mathbf{Z}_c \triangleq (\mathbf{Z}_{c1}^H, \mathbf{Z}_{c2}^H)^H \quad (37)$$

where  $\mathbf{W}_1, \mathbf{C}_1$  and  $\mathbf{Z}_{c1}$  denote the first  $m$  rows of the corresponding matrices. Then the mutual information can be rewritten using the chain rule:

$$\begin{aligned} I(\mathbf{C} + \mathbf{Z}_c; \mathbf{W}) &= I(\mathbf{C}_1 + \mathbf{Z}_{c1}, \mathbf{C}_2 + \mathbf{Z}_{c2}; \mathbf{W}_1, \mathbf{W}_2) \\ &= I(\mathbf{C}_1 + \mathbf{Z}_{c1}; \mathbf{W}_1, \mathbf{W}_2) + I(\mathbf{C}_2 + \mathbf{Z}_{c2}; \mathbf{W}_1, \mathbf{W}_2 | \mathbf{C}_1 + \mathbf{Z}_{c1}) \\ &= I(\mathbf{C}_1 + \mathbf{Z}_{c1}; \mathbf{W}_1) + I(\mathbf{C}_1 + \mathbf{Z}_{c1}; \mathbf{W}_2 | \mathbf{W}_1) \\ &\quad + I(\mathbf{C}_2 + \mathbf{Z}_{c2}; \mathbf{W}_1, \mathbf{W}_2 | \mathbf{C}_1 + \mathbf{Z}_{c1}). \end{aligned} \quad (38)$$

Notice that given  $\mathbf{W}_1, \mathbf{C}_1$  is completely determined. Since the noise  $\mathbf{Z}_{c1}$  is independent of  $\mathbf{W}_2$ , we have  $I(\mathbf{C}_1 + \mathbf{Z}_{c1}; \mathbf{W}_2 | \mathbf{W}_1) = 0$ . By definition,  $I(\mathbf{C}_1 + \mathbf{Z}_{c1}; \mathbf{W}_1) = C(\eta_c, \alpha_{1:m})$ . Thus, we obtain the lower bound:

$$\begin{aligned} I(\mathbf{C} + \mathbf{Z}_c; \mathbf{W}) &= C(\eta_c, \alpha_{1:m}) + \\ &I(\mathbf{C}_2 + \mathbf{Z}_{c2}; \mathbf{W}_1, \mathbf{W}_2 | \mathbf{C}_1 + \mathbf{Z}_{c1}) \geq C(\eta_c, \alpha_{1:m}). \end{aligned} \quad (39)$$

On the other hand, expanding the conditional mutual information with differential entropy yields the upper bound:

$$\begin{aligned} I(\mathbf{C} + \mathbf{Z}_c; \mathbf{W}) &= C(\eta_c, \alpha_{1:m}) + h(\mathbf{C}_2 + \mathbf{Z}_{c2} | \mathbf{C}_1 + \mathbf{Z}_{c1}) \\ &\quad - h(\mathbf{C}_2 + \mathbf{Z}_{c2} | \mathbf{W}_1, \mathbf{W}_2, \mathbf{C}_1 + \mathbf{Z}_{c1}) \\ &\leq C(\eta_c, \alpha_{1:m}) + h(\mathbf{C}_2 + \mathbf{Z}_{c2}) - h(\mathbf{Z}_{c2}). \end{aligned} \quad (40)$$

The inequality holds because conditioning reduces entropy, and given  $\mathbf{W}_1, \mathbf{W}_2$ , the signal part  $\mathbf{C}_2$  is deterministic, leaving only the noise entropy  $h(\mathbf{Z}_{c2})$ .

For  $i > m$ , we have  $\alpha_i \geq 0.5$ , which means  $0.5 - \alpha_i \leq 0$ . Therefore, as  $\eta_c \rightarrow \infty$ , the power of the components in  $\mathbf{C}_2$  is bounded (either staying constant or decaying to zero). Consequently,  $h(\mathbf{C}_2 + \mathbf{Z}_{c2})$  is bounded, making the difference  $h(\mathbf{C}_2 + \mathbf{Z}_{c2}) - h(\mathbf{Z}_{c2})$  bounded by a constant.

Since  $\alpha_{1:m} < 0.5$ ,  $C(\eta_c, \alpha_{1:m}) \rightarrow \infty$  as  $\eta_c \rightarrow \infty$ . Dividing both bounds by  $C(\eta_c, \alpha_{1:m})$  and taking the limit, the bounded term vanishes, leading to:

$$\lim_{\eta_c \rightarrow \infty} \frac{C(\eta_c, \alpha_{1:m})}{I(\mathbf{C} + \mathbf{Z}_c; \mathbf{W})} = 1. \quad (41)$$

$\square$

APPENDIX D  
PROOF OF THEOREM 1

*Proof:* First we prove that  $c_{\eta_c, \alpha} \leq \eta_c^{\alpha_m - 0.5}$ , which is to prove that on the generalized Stiefel manifold  $S_{\eta_c, \alpha}$ , the three corresponding indicators in (16) decline at a speed no less than  $\eta_c^{\alpha_m - 0.5}$ , respectively.

For the sake of brevity, in the following proof, we use the notation

$$\Sigma = \text{diag}(\sigma_1, \dots, \sigma_m) \triangleq \sqrt{\frac{T}{M}} \text{diag}(\eta_c^{0.5 - \alpha_{1:m}}) \quad (42)$$

where  $\sigma_1 \geq \sigma_2 \geq \dots \geq \sigma_m$ . Note that the definitions of  $\Sigma$  and  $\sigma_i$  here differ from the main text. Correspondingly, for arbitrary  $\mathbf{X} \in S_{\eta_c, \alpha}$ .

$$\mathbf{X}\mathbf{X}^H = \Sigma^2. \quad (43)$$

A. *Proof of  $\max_{\Delta \in \mathbb{T}_S S_{\eta_c, \alpha}, g(\Delta, \Delta)=1} |\mathbf{II}_S(\Delta, \Delta)| \doteq \eta_c^{\alpha_m - 0.5}$*

*Proof:* Since  $S_{\eta_c, \alpha}$  is a homogeneous space, we may consider its second fundamental form at arbitrary  $\mathbf{S} \in S_{\eta_c, \alpha}$ . By differentiating (43), the tangent space  $\mathbb{T}_S S_{\eta_c, \alpha}$  at  $\mathbf{S}$  is:

$$\mathbb{T}_S S_{\eta_c, \alpha} = \{ \Delta \in \mathbb{C}^{m \times T}; \mathbf{S}\Delta^H + \Delta\mathbf{S}^H = \mathbf{0} \}. \quad (44)$$

The corresponding normal space at  $\mathbf{S}$  is:

$$\mathbb{N}_S S_{\eta_c, \alpha} = \{ \Gamma\mathbf{S}; \Gamma = \Gamma^H \in \mathbb{C}^{m \times m} \}. \quad (45)$$

which is easy to verify by first left-multiplying  $\Gamma$  on the equation in (44) to get their orthogonality, and then counting two subspaces' dimensions. Without loss of generality, set

$$\mathbf{S} = (\Sigma, \mathbf{0}_{m \times (T-m)}). \quad (46)$$

To calculate  $\mathbf{II}_S(\Delta, \Delta)$ , we consider the unit-speed geodesic  $\gamma(t)$  on  $S_{\eta_c, \alpha}$  starting at  $\gamma(0) = \mathbf{S}$  and initial velocity  $\gamma'(0) = \Delta \in \mathbb{T}_S S_{\eta_c, \alpha}$  with  $g(\Delta, \Delta) = \text{tr}(\Delta\Delta^H) = 1$ . Further differentiating (43) along  $\gamma(t)$  at 0 yields:

$$S\gamma''(0)^H + \gamma''(0)S^H = -2\Delta\Delta^H. \quad (47)$$

Since  $\gamma(t)$  is an embedded geodesic, by basic differential geometry, we have  $\gamma''(0) \perp \mathbb{T}_S S_{\eta_c, \alpha}$ , i.e.  $\gamma''(0) \in \mathbb{N}_S S_{\eta_c, \alpha}$ . By (45), we re-express  $\gamma''(0)$  as:

$$\gamma''(0) = \Gamma\Delta\mathbf{S}, \quad \Gamma\Delta = \Gamma\Delta^H \quad (48)$$

and (47) becomes:

$$S\mathbf{S}^H\Gamma\Delta^H + \Gamma\Delta\mathbf{S}\mathbf{S}^H = \Sigma^2\Gamma\Delta^H + \Gamma\Delta\Sigma^2 = -2\Delta\Delta^H. \quad (49)$$

Since  $\Sigma$  is a diagonal matrix with positive diagonal entries, utilizing (43), one can directly calculate the Hermit matrix  $\Gamma\Delta$  and curvature  $|\gamma''(0)|$  along the geodesic as:

$$(\Gamma\Delta)_{ij} = -\frac{2(\Delta\Delta^H)_{ij}}{\sigma_i^2 + \sigma_j^2} \quad (50)$$

$$\begin{aligned} |\gamma''(0)| &= \sqrt{\text{tr}(\gamma''(0)\gamma''(0)^H)} = \sqrt{\text{tr}(\Gamma\Delta\Sigma^2\Gamma\Delta^H)} \\ &= \sqrt{\sum_{i,j} \sigma_i^2 |(\Gamma\Delta)_{ij}|^2} = \sqrt{\frac{1}{2} \sum_{i,j} (\sigma_i^2 + \sigma_j^2) |(\Gamma\Delta)_{ij}|^2} \\ &= \sqrt{\sum_{i,j} \frac{2|(\Delta\Delta^H)_{ij}|^2}{\sigma_i^2 + \sigma_j^2}} \stackrel{(a)}{\leq} \sqrt{\sum_{i,j} \frac{2(\Delta\Delta^H)_{ii}(\Delta\Delta^H)_{jj}}{\sigma_i^2 + \sigma_j^2}} \end{aligned} \quad (51)$$

where (a) comes from noting that  $\Delta\Delta^H$  is positive semi-definite. denote the diagonal part of  $\Delta\Delta^H$  by  $x_i \triangleq (\Delta\Delta^H)_{ii}$ , we can construct the following optimization problem for an upper bound of  $|\gamma''(0)|$ .

$$\mathcal{P}_{a-1}: \max_{x_i} \sum_{i,j} \frac{2x_i x_j}{\sigma_i^2 + \sigma_j^2} \quad (52a)$$

$$\text{s.t.} \quad \sum_i x_i = 1, \quad x_i \leq 0. \quad (52b)$$

Note that (52a) is a quadratic form, and using the fact that the matrix constructed by  $1/(\sigma_i^2 + \sigma_j^2)$  is positive semi-definite, the optimization function (52a) is convex. Since the feasible region (52b) form a simplex in  $\mathbb{R}^m$ , thus the optimal  $(x_{1,opt}, \dots, x_{m,opt})$  lies on the simplex's corners, i.e.  $x_{k,opt} = 1$  for some  $k \in [1, m]$ . Since  $\sigma_i$  is non-increasing by  $i$ , the solution to  $\mathcal{P}_{a-1}$  is  $1/\sigma_m^2$  by setting  $x_m = 1$ .

Combining the solution for  $\mathcal{P}_{a-1}$  and (51) yields an upper bound for  $|\gamma''(0)|$ , i.e.

$$|\gamma''(0)| \leq \frac{1}{\sigma_m}. \quad (53)$$

Furthermore, the upper bound is tight. It can be achieved by choosing initial velocity  $\gamma'(0) = \Delta_m \in \mathbb{T}_S S_{\eta_c, \alpha}$  s.t.

$$\Delta_m = \begin{pmatrix} \mathbf{0}_{(m-1) \times m} & \mathbf{0}_{(m-1) \times (T-m)} \\ \mathbf{0}_{1 \times m} & \mathbf{u} \end{pmatrix} \quad (54)$$

with  $\mathbf{u}\mathbf{u}^H = 1$ . By the Gauss formula along a curve [13, Co. 8.3], since  $\gamma(t)$  is a unit speed geodesic, we have:

$$\mathbf{II}_S(\Delta, \Delta) = \gamma''(0). \quad (55)$$

Therefore, we arrive at the desired expression:

$$\begin{aligned} \max_{\Delta \in \mathbb{T}_S S_{\eta_c, \alpha}, g(\Delta, \Delta)=1} |\mathbf{II}_S(\Delta, \Delta)| &= \sqrt{\frac{M}{T}} \eta_c^{\alpha_m - 0.5} \\ &\doteq \eta_c^{\alpha_m - 0.5}. \end{aligned} \quad (56)$$

□

B. *Proof of  $\rho_{\perp}(S_{\eta_c, \alpha})^{-1} \leq \eta_c^{\alpha_m - 0.5}$*

*Proof:* Since  $S_{I_m}^{(m,T)}$  is compact, there exists a uniform tubular neighborhood around  $S_{I_m}^{(m,T)}$  [13, Thm. 5.25]. To prove the desired inequality, we show that a uniform tubular neighborhood around  $S_{\eta_c, \alpha}$  exists with radius  $r = \sigma_m$ . For arbitrary

$$\mathbf{S} = \Sigma\mathbf{U} \in S_{\eta_c, \alpha}, \mathbf{U} \in S_{I_m}^{(m,T)}. \quad (57)$$

Utilizing the normal space (45), we construct the Fermi coordinate representation of the tubular neighborhood by choosing  $\Gamma = \Gamma^H$  and let

$$\mathbf{X} = \mathbf{S} + \Gamma \mathbf{S} = (\mathbf{I} + \Gamma) \Sigma \mathbf{U} \quad (58)$$

and the uniform tubular neighborhood  $T(S_{\eta_c, \alpha}, r)$  around  $S_{\eta_c, \alpha}$  of radius  $r$  is:

$$T(S_{\eta_c, \alpha}, r) = \{( \mathbf{I} + \Gamma) \Sigma \mathbf{U}; \mathbf{U} \mathbf{U}^H = \mathbf{I}_m, \Gamma = \Gamma^H, \|\Gamma \Sigma \mathbf{U}\|_F < r\} \quad (59)$$

To show that  $T(S_{\eta_c, \alpha}, \sigma_m)$  is indeed a tubular neighborhood, using the theorem of invariance of domain one needs to prove (58) is a injection. Consider the Euclidean projection of  $\mathbf{X} \in T(S_{\eta_c, \alpha}, r)$  to  $S_{\eta_c, \alpha}$ , i.e. the following optimization problem

$$\mathcal{P}_{a-2} : \min_{\tilde{\mathbf{U}}} \|( \mathbf{I} + \Gamma) \Sigma \mathbf{U} - \Sigma \tilde{\mathbf{U}}\|_F \quad (60a)$$

$$\text{s.t. } \tilde{\mathbf{U}} \tilde{\mathbf{U}}^H = \mathbf{I}_m. \quad (60b)$$

Minimizing (60a) is equivalent to maximizing

$$\max_{\tilde{\mathbf{U}}} \Re \left\{ \text{tr} \left[ (\mathbf{I} + \Gamma) \Sigma \mathbf{U} \tilde{\mathbf{U}}^H \Sigma \right] \right\} \quad (60c)$$

$$= \Re \left\{ \text{tr} \left[ \Sigma (\mathbf{I} + \Gamma) \Sigma \mathbf{U} \tilde{\mathbf{U}}^H \right] \right\}. \quad (60d)$$

Since  $\|\Gamma \Sigma \mathbf{U}\|_F \leq \sigma_m$ , using the fact  $0 \leq \sigma_m \leq \sigma_i$ , we have

$$\sigma_m^2 \text{tr}(\Gamma \Gamma^H) \leq \text{tr}(\Gamma \Sigma^2 \Gamma^H) < \sigma_m^2 \quad (61)$$

therefore any eigenvalue  $\lambda(\Gamma)$  of  $\Gamma$ ,

$$|\lambda(\Gamma)| < 1, \quad \Sigma(\mathbf{I} + \Gamma)\Sigma \succ \Sigma(\mathbf{I} - \Gamma)\Sigma = \mathbf{0} \quad (62)$$

and let  $\Sigma(\mathbf{I} + \Gamma)\Sigma = \mathbf{U}_1 \mathbf{A}_1 \mathbf{U}_1^H$  be the eigenvalue decomposition, the optimization objective (60d) further becomes:

$$\max_{\tilde{\mathbf{U}}} \Re \left\{ \text{tr} \left( \mathbf{A}_1 \mathbf{U}_1^H \mathbf{U} \tilde{\mathbf{U}}^H \mathbf{U}_1 \right) \right\}. \quad (63)$$

Since  $\mathbf{A}_1 \succ \mathbf{0}$  and  $\mathbf{U}_1^H \mathbf{U} \tilde{\mathbf{U}}^H \mathbf{U}_1$  is also unitary, it is trivial that the only solution to  $\mathcal{P}_{a-2}$  is

$$\mathbf{U}_1^H \mathbf{U} \tilde{\mathbf{U}}^H \mathbf{U}_1 = \mathbf{I}, \quad \text{i.e. } \tilde{\mathbf{U}} = \mathbf{U}. \quad (64)$$

That is, arbitrary matrix  $\mathbf{X} = \mathbf{S} + \Gamma \mathbf{S} \in T(S_{\eta_c, \alpha}, r)$  has unique Euclidean projection  $\mathbf{S}$  w.r.t.  $S_{\eta_c, \alpha}$ . If  $\mathbf{X}$  can also be expressed as  $\mathbf{X} = \mathbf{S}_1 + \Gamma_1 \mathbf{S}_1$ , the uniqueness of the Euclidean projection doesn't hold. Therefore  $T(S_{\eta_c, \alpha}, \sigma_m)$  is a uniform tubular neighborhood indeed. And we arrive at:

$$\rho_{\perp}(S_{\eta_c, \alpha})^{-1} \leq \frac{1}{\sigma_m} = \sqrt{\frac{M}{T}} \eta_c^{\alpha_m - 0.5} \doteq \eta_c^{\alpha_m - 0.5}. \quad (65)$$

C. Proof of  $\rho_{\top}(S_{\eta_c, \alpha})^{-1} \leq \eta_c^{\alpha_m - 0.5}$

*Proof:* To prove the desired inequality, we use the following celebrated Klingenberg's Theorem:

*Lemma 3 (Klingenberg):* Let  $(M, g)$  be a compact Riemannian manifold whose sectional curvature satisfies  $K \leq C$  for some constant  $C$ . Then either

$$\rho_{\top}(M) \geq \frac{\pi}{\sqrt{C}} \quad (66)$$

or there exists a closed geodesic  $\gamma$  in  $M$  whose length is minimum among all closed geodesics, such that

$$\rho_{\top}(M) = \frac{1}{2} L(\gamma). \quad (67)$$

Since  $S_{\eta_c, \alpha}$  is compact, Lemma 3 is suitable, thus we focus on the upper bound of the sectional curvature  $K$  and the minimum distance  $L(\gamma)$  of a closed geodesic  $\gamma$  on  $S_{\eta_c, \alpha}$ .

First, note that the sectional curvature  $K$  is bounded by:

$$K = g(\mathbf{\Pi}_S(\Delta_1, \Delta_1), \mathbf{\Pi}_S(\Delta_2, \Delta_2)) \leq \max_{\Delta} |\mathbf{\Pi}_S(\Delta, \Delta)|^2 \quad (68)$$

where unit tangent vectors  $\Delta_1, \Delta_2, \Delta \in \mathbb{T}_S S_{\eta_c, \alpha}$  with  $\Delta_1 \perp \Delta_2$ .

Second, for arbitrary closed geodesic  $\gamma(t)$  in  $S_{\eta_c, \alpha}$ , according to the analysis in Section D-A, we have:

$$|\gamma''(t)| = |\mathbf{\Pi}_{\gamma(t)}(\gamma'(t), \gamma'(t))| \leq \frac{1}{\sigma_m} \quad (69)$$

therefore, for  $\gamma$  to be closed, we have

$$L(\gamma) \leq \frac{2\pi}{\sigma_m}. \quad (70)$$

Therefore, combining (56), (68) and (70), Lemma 3 yields our desired result

$$\rho_{\top}(S_{\eta_c, \alpha})^{-1} \leq \eta_c^{\alpha_m - 0.5}. \quad (71)$$

□

Combining these results, we arrive at:

$$c_{\eta_c, \alpha} \leq \eta_c^{\alpha_m - 0.5} \quad (72)$$

substituting the inequality to (17) and focusing on its RHS, if  $\alpha_m \leq 0$ , the RHS obviously converges to zero as  $\eta_c \rightarrow \infty$ , if  $\alpha_m > 0$ , we have:

$$\begin{aligned} & \lim_{\eta_c \rightarrow \infty} \delta^{-1} (1 + c_{\eta_c, \alpha} \eta_c^{0.5})^{\delta} c_{\eta_c, \alpha}^2 \log^2(c_{\eta_c, \alpha}) \\ &= \lim_{\eta_c \rightarrow \infty} \delta^{-1} (1 + \eta_c^{\alpha_m})^{\delta} \eta_c^{2\alpha_m - 1} \log^2(\eta_c^{2\alpha_m - 1}) \\ &= \lim_{\eta_c \rightarrow \infty} (\delta(2\alpha_m - 1))^{-1} \eta_c^{(2+\delta)\alpha_m - 1} \log^2(\eta_c) \\ &\stackrel{(a)}{=} 0 \end{aligned} \quad (73)$$

where (a) comes from choosing  $0 < \delta < 1/\alpha_m - 2$ . Thus by inequality (17), we have

$$\lim_{\eta_c \rightarrow \infty} |h(\mathbf{C}_1 + \mathbf{Z}_{c1}) - m^2 \log(\pi e) - \log \text{Vol}(S_{\eta_c, \alpha})| \quad (74)$$

□

$$f_u(\mathbf{s})dV_1|_{u(\mathbf{s})} = \phi^*dV_2|_{\phi \circ u(\mathbf{s})} = \phi^*dV_2|_{u \circ \phi(\mathbf{s})} = (u \circ u^{-1} \circ \phi)^*dV_2|_{u \circ \phi(\mathbf{s})} = (u^{-1} \circ \phi)^*dV_2|_{\phi(\mathbf{s})} = (u^{-1})^*f_{\mathbf{S}}dV_1|_{\mathbf{S}} = f_{\mathbf{S}}dV_1|_{u(\mathbf{s})} \quad (79)$$

$$f = f dV_1(\mathbf{V}_{1:5}) = \phi^*dV_2(\mathbf{V}_{1:5}) = dV_2(\phi_*(\mathbf{V}_{1:5})) = dV_2\left(\sqrt{\frac{\sigma_i^2 + \sigma_j^2}{2}} \mathbf{W}_{1,2,ij}, \sigma_i \mathbf{W}_{3:5,ij}\right) = 2^{-\frac{m(m-1)}{2}} \prod_{i < j} (\sigma_i^2 + \sigma_j^2) \prod_i \sigma_i^{2T-2m+1} \quad (80)$$

$$\lim_{\eta_c \rightarrow \infty} \left| h(\mathbf{C}_1 + \mathbf{Z}_{c1}) - \frac{m^2}{2} \log(\pi e) - \log \left( 2^{-\frac{m(m-1)}{2}} \prod_{i < j} (\sigma_i^2 + \sigma_j^2) \prod_i \sigma_i^{2T-2m+1} \prod_{i=T-m+1}^T \frac{2\pi^i}{(i-1)!} \right) \right| = 0 \quad (81)$$

$$\lim_{\eta_c \rightarrow \infty} \left| I_{\mathbf{H}_c}(\mathbf{X}; \mathbf{Y}_c) - \frac{m(2T-m)}{2} \log(\pi e) - \log \left( 2^{-\frac{m(m-1)}{2}} \prod_{i < j} (\sigma_i^2 + \sigma_j^2) \prod_i \sigma_i^{2T-2m+1} \prod_{i=T-m+1}^T \frac{2\pi^i}{(i-1)!} \right) \right| = 0 \quad (82)$$

Next, we show that

$$\text{Vol}(S_{\eta_c, \alpha}) = 2^{-\frac{m(m-1)}{2}} \prod_{i < j} (\sigma_i^2 + \sigma_j^2) \prod_i \sigma_i^{2T-2m+1} \text{Vol}(S_{\mathbf{I}_m}^{(m,T)}) \quad (75)$$

where

$$\text{Vol}(S_{\mathbf{I}_m}^{(m,T)}) = \prod_{i=T-m+1}^T \frac{2\pi^i}{(i-1)!} \quad (76)$$

is the Euclidean volume of a standard Complex Stiefel manifold [14].

#### D. Proof of (75)

*Proof:* Consider the diffeomorphism

$$\phi : S_{\mathbf{I}_m}^{(m,T)} \rightarrow S_{\eta_c, \alpha}, \quad \mathbf{X} \mapsto \Sigma \mathbf{X} \quad (77)$$

Let  $dV_1$  and  $dV_2$  denote the Euclidean Riemannian volume form on  $S_{\mathbf{I}_m}^{(m,T)}$  and  $S_{\eta_c, \alpha}$ , respectively. By definition:

$$\text{Vol}(S_{\eta_c, \alpha}) = \int_{S_{\eta_c, \alpha}} dV_2 = \int_{S_{\mathbf{I}_m}^{(m,T)}} \phi^* dV_2 = \int_{S_{\mathbf{I}_m}^{(m,T)}} f dV_1 \quad (78)$$

for some function  $f$  on  $S_{\mathbf{I}_m}^{(m,T)}$ , where  $\phi^*$  denotes the pull-back operation of differential forms. Since both manifolds are  $U(T)$ -homogeneous, and utilizing associative property of matrix multiplication, for arbitrary  $\mathbf{U} \in U(T)$ , let  $u : \mathbf{X} \mapsto \mathbf{X}\mathbf{U}$ , for arbitrary  $\mathbf{S} \in S_{\mathbf{I}_m}^{(m,T)}$ , equation (D-D) holds, thus  $f$  is a constant on  $S_{\mathbf{I}_m}^{(m,T)}$ .

Without loss of generality, we consider  $f$  at

$$\mathbf{S} = (\mathbf{I}_m, \mathbf{0}_{m \times (T-m)}), \phi(\mathbf{S}) = (\Sigma, \mathbf{0}_{m \times (T-m)}) \quad (83)$$

and find the orthonormal basis for  $\mathbb{T}_{\mathbf{S}} S_{\mathbf{I}_m}^{(m,T)}$  and  $\mathbb{T}_{\phi(\mathbf{S})} S_{\eta_c, \alpha}$ . Specifically, the following tangent matrices form a orthonormal

basis for  $\mathbb{T}_{\mathbf{S}} S_{\mathbf{I}_m}^{(m,T)}$ :

$$\mathbf{V}_{1,ij} = \left( \frac{1}{\sqrt{2}} (\mathbf{E}_{ij} - \mathbf{E}_{ji}), \mathbf{0}_{m \times (T-m)} \right), \quad i < j \quad (84a)$$

$$\mathbf{V}_{2,ij} = \sqrt{-1} \left( \frac{1}{\sqrt{2}} (\mathbf{E}_{ij} + \mathbf{E}_{ji}), \mathbf{0}_{m \times (T-m)} \right), \quad i < j \quad (84b)$$

$$\mathbf{V}_{3,i} = \sqrt{-1} (\mathbf{E}_{ii}, \mathbf{0}_{m \times (T-m)}) \quad (84c)$$

$$\mathbf{V}_{4,ij} = (\mathbf{0}_{m \times m}, \mathbf{E}_{ij}) \quad (84d)$$

$$\mathbf{V}_{5,ij} = \sqrt{-1} (\mathbf{0}_{m \times m}, \mathbf{E}_{ij}) \quad (84e)$$

and we organize them as  $\mathbf{V}_{1:5}$ . Similarly, a set of orthonormal basis for  $\mathbb{T}_{\phi(\mathbf{S})} S_{\eta_c, \alpha}$  is:

$$\mathbf{W}_{1,ij} = \left( \frac{\sigma_i \mathbf{E}_{ij} - \sigma_j \mathbf{E}_{ji}}{\sqrt{\sigma_i^2 + \sigma_j^2}}, \mathbf{0}_{m \times (T-m)} \right), \quad i < j \quad (85a)$$

$$\mathbf{W}_{2,ij} = \sqrt{-1} \left( \frac{\sigma_i \mathbf{E}_{ij} + \sigma_j \mathbf{E}_{ji}}{\sqrt{\sigma_i^2 + \sigma_j^2}}, \mathbf{0}_{m \times (T-m)} \right), \quad i < j \quad (85b)$$

$$\mathbf{W}_{3,i} = \sqrt{-1} (\mathbf{E}_{ii}, \mathbf{0}_{m \times (T-m)}) \quad (85c)$$

$$\mathbf{W}_{4,ij} = (\mathbf{0}_{m \times m}, \mathbf{E}_{ij}) \quad (85d)$$

$$\mathbf{W}_{5,ij} = \sqrt{-1} (\mathbf{0}_{m \times m}, \mathbf{E}_{ij}) \quad (85e)$$

$$\quad (85f)$$

Therefore we have:

$$\phi_*(\mathbf{V}_{1,2,ij}) = \Sigma \mathbf{V}_{1,2,ij} = \sqrt{\frac{\sigma_i^2 + \sigma_j^2}{2}} \mathbf{W}_{1,2,ij} \quad (86a)$$

$$\phi_* \mathbf{V}_{3:5,ij} = \Sigma \mathbf{V}_{3:5,ij} = \sigma_i \mathbf{W}_{3:5,ij} \quad (86b)$$

where  $\phi_*$  denotes the push-forward of tangent vectors, thus  $f$  can be calculated by (80). The desired (75) then comes from using (78).  $\square$

Substituting our results into (42) yields the asymptotic differential entropy and mutual information in (81) and (82).

Utilizing (42) and the fact that  $\alpha_i \leq \alpha_{i+1}$ , for  $i < j$ , we have

$$(\sigma_i^2 + \sigma_j^2) \doteq \eta_c^{1-2\alpha_i} \quad (87)$$

and the asymptotic entropy and mutual information is thus:

$$\begin{aligned} I_{\mathbf{H}_c}(\mathbf{X}; \mathbf{Y}_c) &\doteq h_{\alpha}(\mathbf{C}_1 + \mathbf{Z}_{c1}) \\ &\doteq \sum_{i=1}^{\text{rk}(\mathbf{R})} (2T + 1 - 2i)(0.5 - \alpha_i)^+ \log(\eta_c). \end{aligned} \quad (88)$$

□

## APPENDIX E PROOF OF LEMMA 2

### A. Proof of (26)

*Proof:* Let the eigendecomposition of the transmit covariance be  $\mathbf{R} = \mathbf{U}\mathbf{A}\mathbf{U}^H$ , with  $\mathbf{A} = \text{diag}(\lambda_1, \lambda_2, \dots, \lambda_{\text{rk}(\mathbf{R})}, 0, \dots, 0) \triangleq \text{diag}(\boldsymbol{\lambda}^T, 0, \dots, 0)$ . Since elements of  $\mathbf{H}_c$  are i.i.d. white complex Gaussian distributed and  $\mathbf{U} \in U(M)$ , let  $\mathbf{A}_{>0} = \text{diag}(\boldsymbol{\lambda})$ , we have:

$$\mathbf{H}_c \mathbf{R} \mathbf{H}_c^H = \mathbf{H}_c \mathbf{U} \mathbf{A} \mathbf{U}^H \mathbf{H}_c^H \sim \mathbf{H}_c \mathbf{A} \mathbf{H}_c^H = \mathbf{H}_{c1} \mathbf{A}_{>0} \mathbf{H}_{c1}^H \quad (89)$$

where  $\mathbf{H}_{c1}$  denotes the first  $\text{rk}(\mathbf{R})$  columns of  $\mathbf{H}_c$ . Since  $\mathbf{H}_{c1} \mathbf{A}_{>0} \mathbf{H}_{c1}^H = (\mathbf{A}_{>0}^{1/2} \mathbf{H}_{c1}^H)^H (\mathbf{A}_{>0}^{1/2} \mathbf{H}_{c1}^H)$  has the same eigenvalues as  $(\mathbf{A}_{>0}^{1/2} \mathbf{H}_{c1}^H) (\mathbf{A}_{>0}^{1/2} \mathbf{H}_{c1}^H)^H$ , one only needs to consider the eigenvalue distribution of

$$(\mathbf{A}_{>0}^{1/2} \mathbf{H}_{c1}^H) (\mathbf{A}_{>0}^{1/2} \mathbf{H}_{c1}^H)^H \sim \mathcal{W}_{\text{rk}(\mathbf{R})}(N_c, \mathbf{A}_{>0}) \quad (90)$$

where the RHS stands for the central complex Wishart distribution with  $N_c$  degrees of freedom and covariance matrix  $\mathbf{A}_{>0}$ . The eigenvalue distribution of such a random matrix is [15]:

$$\frac{\det(\{e^{-a_j/\lambda_i}\})}{\det \mathbf{A}_{>0}^{N_c}} \prod_{\ell=1}^{\text{rk}(\mathbf{R})} \frac{a_{\ell}^{N_c - \text{rk}(\mathbf{R})}}{(N_c - \ell)!} \prod_{k < \ell} \frac{a_k - a_{\ell}}{\lambda_k - \lambda_{\ell}} \lambda_{\ell} \lambda_k. \quad (91)$$

where  $a_i = \sigma_i^2$  are the eigenvalues. We arrive at (26) by utilizing change of variables:

$$\alpha_i = -\frac{\log a_i}{2 \log \eta_c} \quad (92)$$

and accounting for the Jacobian determinant. □

### B. Proof of (27)

*Proof:* First, we focus on the part  $\alpha_1 > 0$ , i.e.  $\alpha_i > 0$  for arbitrary  $i \in \{1, 2, \dots, \text{rk}(\mathbf{R})\}$ . Again, let  $x_i = \eta_c^{-2\alpha_i}$ , as  $\eta_c \rightarrow \infty$ ,  $x_i \rightarrow 0^+$ , we have

$$p(\boldsymbol{\alpha}) \propto \det \left( \left\{ \frac{e^{-x_i}}{\lambda_j} \right\} \right) \prod_{m=1}^{\text{rk}(\mathbf{R})} x_m^{(N_c - \text{rk}(\mathbf{R}) + 1)} \prod_{k < l}^{\text{rk}(\mathbf{R})} (x_k - x_l) \quad (93)$$

focusing on the first term  $\det \left( \left\{ \frac{e^{-x_i}}{\lambda_j} \right\} \right)$  on the RHS, as  $x_i \rightarrow 0^+$ , we have

$$\begin{aligned} &\det \left( \left\{ \frac{e^{-x_i}}{\lambda_j} \right\} \right) \\ &= \det \left( \left\{ \sum_{k=0}^{\text{rk}(\mathbf{R})-1} \left( \frac{(-1)^k}{\lambda_j} \frac{1}{k!} x_i^k \right) (1 + o(1)) \right\} \right) \\ &= \det \left( \left\{ \sum_{k=0}^{\text{rk}(\mathbf{R})-1} \frac{(-1)^k}{\lambda_j} \frac{1}{k!} \right\} \right) \det(\{x_i^k\}) (1 + o(1)) \\ &\propto \prod_{k < l}^{\text{rk}(\mathbf{R})} (x_k - x_l) (1 + o(1)). \end{aligned} \quad (94)$$

Therefore,

$$\begin{aligned} p(\boldsymbol{\alpha}) &\propto \prod_{m=1}^{\text{rk}(\mathbf{R})} x_m^{(N_c - \text{rk}(\mathbf{R}) + 1)} \prod_{k < l}^{\text{rk}(\mathbf{R})} (x_k - x_l)^2 \\ &\doteq \eta_c^{-\sum_{i=1}^{\text{rk}(\mathbf{R})} 2(N_c + \text{rk}(\mathbf{R}) + 1 - 2i)\alpha_i}. \end{aligned} \quad (95)$$

and the first part of (27) is proved.

For the other part, if  $\alpha_1 < 0$ , by the decomposition law for determinants, the determinant term  $\det \left( \left\{ \frac{e^{-\eta_c^{-2\alpha_i}}}{\lambda_j} \right\} \right)$  in (93) becomes

$$\sum_k^{\text{rk}(\mathbf{R})} (-1)^{k+1} \frac{e^{-\eta_c^{-2\alpha_1}}}{\lambda_k} \det_{i \neq 1, j \neq k} \left( \left\{ \frac{e^{-\eta_c^{-2\alpha_i}}}{\lambda_j} \right\} \right). \quad (96)$$

It is then trivial that  $p(\boldsymbol{\alpha})$  scales with  $\eta_c$  faster than  $e^{-\eta_c^{-2\alpha_1}}$ , thus yielding the desired

$$\lim_{\eta_c \rightarrow \infty} \frac{\log p_{\boldsymbol{\alpha}}(\boldsymbol{\alpha})}{\log \eta_c} = -\infty. \quad (97)$$

□

## APPENDIX F PROOF OF THEOREM 2

*Proof:* To find  $d_{\text{rk}(\mathbf{R})}^{\text{out}}(r)$  is to find the solution for the following optimization problem:

$$\mathcal{P}_{a-3} : \min_{\boldsymbol{\alpha}} 2 \left( \sum_{i=1}^{\text{rk}(\mathbf{R})} (N_c + \text{rk}(\mathbf{R}) + 1 - 2i)\alpha_i \right) \quad (98a)$$

$$\text{s.t.} \quad \sum_i^{\text{rk}(\mathbf{R})} (2T + 1 - 2i)(0.5 - \alpha_i)^+ \leq Tr \quad (98b)$$

$$0 \leq \alpha_1 \leq \alpha_2 \leq \dots \leq \alpha_{\min\{N_c, \text{rk}(\mathbf{R})\}} \quad (98c)$$

where (98a) is  $d_{\text{rk}(\mathbf{R})}^{\text{out}}(r)$ . Similar to the approach in [6], notice that the optimal solution for  $r = k(1 - \frac{k}{2T}) \triangleq r(k)$  is

$$\alpha_i = \begin{cases} 0, & 1 \leq i \leq k \\ 0.5, & k < i \leq \text{rk}(\mathbf{R}). \end{cases} \quad (99)$$

with  $d_{\text{rk}(\mathbf{R})}^{\text{out}}(r(k))$  being:

$$\begin{aligned} d_{\text{rk}(\mathbf{R})}^{\text{out}}(r(k)) &= \sum_{i=k+1}^{\text{rk}(\mathbf{R})} (N_c + \text{rk}(\mathbf{R}) + 1 - 2i) \\ &= (N_c - k)(\text{rk}(\mathbf{R}) - k). \end{aligned} \quad (100)$$

For other  $r$ , as  $r$  grows from  $r(k)$  to  $r(k) < r < r(k+1)$ , the optimal  $\alpha_{k+1}$  grows from 0 towards 0.5. It follows easily that the corresponding  $d_{\text{rk}(\mathbf{R})}^{\text{out}}(r)$  is the affine combination of  $d_{\text{rk}(\mathbf{R})}^{\text{out}}(k)$  and  $d_{\text{rk}(\mathbf{R})}^{\text{out}}(k+1)$  as (98a) is linear in  $\alpha$ .

After obtaining the outage probability, the outage bound (30) can be proved using the same proof as [6, Lem. 5] thus we omit the derivation for brevity.  $\square$